

Cite this: *Dalton Trans.*, 2023, **52**,  
3725From ferrocene to decasubstituted enantiopure  
ferrocene-1,1'-disulfoxide derivatives†Min Wen,<sup>a</sup> William Erb,<sup>b</sup> Florence Mongin,<sup>a</sup> Jean-Pierre Hurvois,<sup>a</sup>  
Yury S. Halauko,<sup>\*b</sup> Oleg A. Ivashkevich,<sup>c</sup> Vadim E. Matulis,<sup>b</sup> Marielle Blot<sup>a</sup> and  
Thierry Roisnel<sup>†a</sup>

The functionalization of (*R,R*)-*S,S'*-di-*tert*-butylferrocene-1,1'-disulfoxide by deprotolithiation-electrophilic trapping sequences was studied towards polysubstituted, enantiopure derivatives for which the properties were determined. While the 2,2'-disubstituted ferrocene derivatives were obtained as expected, subsequent functionalization of the 2,2'-di(phenylthio) and 2,2'-bis(trimethylsilyl) derivatives occurred primarily at the 4- or 4,4'-positions. This unusual regioselectivity was discussed in detail in light of  $pK_a$  values and structural data. The less sterically hindered 2,2'-difluorinated derivative yielded the expected 1,1',2,2',3,3'-hexasubstituted ferrocenes by the deprotometallation-trapping sequence. Further functionalization proved possible, leading to early examples of 1,1',2,2',3,3',4,4'-octa, nona and even decasubstituted ferrocenes. Some of the newly prepared ferrocene-1,1'-disulfoxides were tested as ligands for enantioselective catalysis and their electrochemical properties were investigated.

Received 25th October 2022,  
Accepted 20th February 2023

DOI: 10.1039/d2dt03456e

rsc.li/dalton

## Introduction

In 70 years,<sup>1,2</sup> ferrocenes have risen to an important place among the different families of organometallic compounds. This stems from the good stabilities towards air, water, heat and light, combined with the reversible redox behaviour of these sandwich compounds.<sup>3</sup> The specific physical and chemical properties that a ferrocene can impart to molecules have allowed applications in various fields<sup>4</sup> such as catalysis,<sup>5-7</sup> medicinal chemistry<sup>8-12</sup> and materials science.<sup>13-16</sup> Since these properties can be tuned by the rational addition of selected substituents, there is a need for synthetic strategies that allow access to functionalized ferrocenes, including enantiopure derivatives.

Since the discovery of ferrocene,<sup>1,2</sup> many mono, 1,2- and 1,1'-disubstituted derivatives have been synthesized.<sup>17-23</sup>

However, other substitution patterns and more substituted derivatives have been significantly less studied.<sup>17-22,24,25</sup>

Among the highly substituted ferrocenes already described, those containing five identical substituents on the same cyclopentadienyl (*e.g.* Me,<sup>26,27</sup> *cPr*,<sup>28</sup> benzyl,<sup>29</sup> ethynyl,<sup>30</sup> Ph,<sup>31</sup> allyl,<sup>32</sup> F,<sup>33,34</sup> Cl,<sup>35,36</sup> Br,<sup>30,37-40</sup> I,<sup>37,38</sup> SMe,<sup>41</sup> SPh<sup>41</sup>) are well represented although they do not offer a high degree of property tuning. Regarding decasubstituted ferrocenes, most representatives with two (*e.g.* Me/phosphine,<sup>42,43</sup> Me/ketone,<sup>44,45</sup> Me/benzyl,<sup>29</sup> Me/alkylthio,<sup>42,46</sup> Cl/SMe<sup>47</sup>) or three<sup>48,49</sup> different substituents are achiral compounds. Moreover, if chiral decasubstituted ferrocenes have been reported once, it is only in the form of racemic mixtures.<sup>50</sup>

As the controlled introduction of substituents on ferrocene allows to modulate its electronic<sup>51-53</sup> and steric<sup>54,55</sup> properties, being able to access hetero-polysubstituted derivatives should provide an unprecedented tuning of properties. Moreover, for potential applications in catalysis, medicinal chemistry or sensing, it is necessary to develop access to enantiopure polysubstituted ferrocenes.

Diastereoselective deprotometallation of a chiral directing group (DG)-substituted ferrocene currently represents the most general approach to access enantiopure 1,2-disubstituted ferrocenes.<sup>18,20,56-58</sup> These can be further functionalized to various tri, tetra and even pentasubstituted ferrocenes. The enantiopure 1,2,3-tri and 1,2,3,4-tetrasubstituted ferrocenes have generally been obtained by successive functionalization of the positions adjacent to the chiral DG which can be for example (*R*)- $\alpha$ -(dimethylamino)ethyl,<sup>59-61</sup> (*S*)-(2-methoxy-

<sup>a</sup>Univ Rennes, CNRS, ISCR (Institut des Sciences Chimiques de Rennes) – UMR 6226, F-35000 Rennes, France. E-mail: william.erb@univ-rennes1.fr

<sup>b</sup>Department of Chemistry, Belarusian State University, 4 Nezavisimosti Av., 220030 Minsk, Belarus. E-mail: hys@tut.by

<sup>c</sup>Laboratory for Chemistry of Condensed Systems, Research Institute for Physical Chemical Problems of Belarusian State University, 14 Leningradskaya St., 220030 Minsk, Belarus

†Electronic supplementary information (ESI) available: Compound synthesis and analysis, NMR spectra, selected NMR NOESY correlations, HPLC data, computational details, lithium stabilization effect, Cartesian coordinates of DFT optimized structures, additional  $pK_a$  values, voltammograms, additional plots. CCDC 2204517–2204523 and 2236043. For ESI and crystallographic data in CIF or other electronic format see DOI: <https://doi.org/10.1039/d2dt03456e>



methyl-1-pyrrolidyl)methyl,<sup>62</sup> (*S*)-4-isopropylloxazoline,<sup>63,64</sup> or the acetal developed by Kagan<sup>55,65–68</sup> (Fig. 1a).

A fourth substituent can also be introduced next to the best DG, as shown by Top, Jaouen<sup>69</sup> and Pugin<sup>60</sup> (Fig. 1b). It should be noted that the substituents can be placed differently if the first substituent introduced is more directing than the chiral group (e.g. Br<sup>60,61,70,71</sup> or (*R*)-*tert*-butylsulfinyl<sup>72</sup> vs. (*R*)- $\alpha$ -(dimethylamino)ethyl, and (*R*)-4-tolylsulfinyl<sup>69</sup> vs. Kagan's acetal; Fig. 1c). This strategy was exploited in our group to introduce successively, on the amine developed by Ugi,<sup>73</sup> Cl, F, I and, after iodine migration,<sup>22,74</sup> SiMe<sub>3</sub> (Fig. 1d).<sup>75</sup>

Sulfoxides are one of the most important chiral groups able to direct a diastereoselective deprotonation. Originally reported by Kagan and co-workers in 1993,<sup>76,77</sup> the 4-tolyl<sup>69,78,79</sup> and *tert*-butylsulfinyl<sup>72</sup> groups are the most employed since they can then be converted by reduction to sulfides<sup>70,78,80–82</sup> or oxidation to sulfones,<sup>83</sup> by sulfoxide/lithium exchange followed by trapping,<sup>69,78,79</sup> or simply removed.<sup>72</sup> Their use to access polyfunctionalized ferrocenes is therefore not surprising.

While Kagan and co-workers chose in 1993 to oxidize the sulfoxide to the sulfone in order to introduce a third substituent<sup>76</sup> (Fig. 2a), we recently showed that the least activated position next to the sulfoxide could be directly functionalized<sup>84,85</sup> (Fig. 2b). As demonstrated by Weissensteiner and co-workers,<sup>61,70</sup> it is also possible to introduce Br and CHO in 2 and 3 position, respectively, taking advantage of the directing group properties of the former (Fig. 2c). Finally, by protecting the most reactive position next to the sulfoxide with a trimethylsilyl, we succeeded in synthesizing the first hetero-1,2,3,4,5-pentasubstituted ferrocene by successive introduction of F, Me and, after deprotection, Cl and SiMe<sub>3</sub><sup>85</sup> (Fig. 2d).

In this article, we report how the wise choice of substituents can allow variously functionalized, especially decasubstituted, ferrocenesulfoxides to be delivered as enantiopure products.

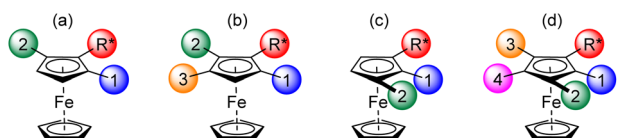


Fig. 1 Already reported enantiopure ferrocenes with three, four or five different substituents and their introduction order.

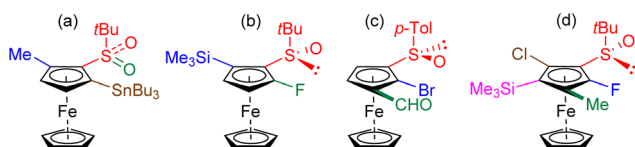


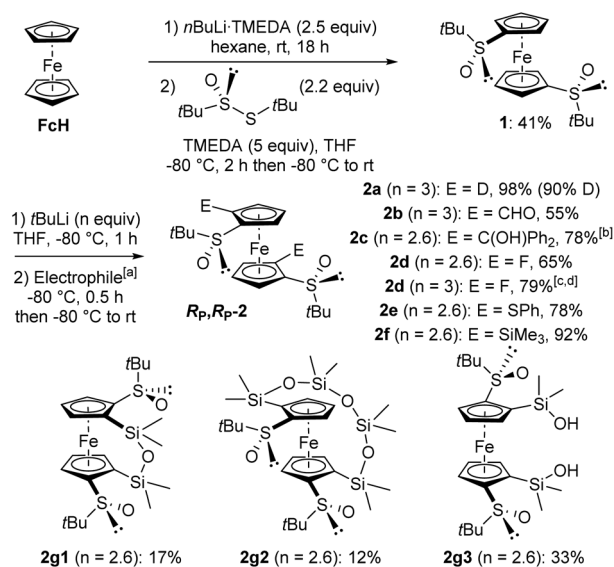
Fig. 2 Use of a chiral sulfoxide to access enantiopure ferrocenes with three or five different substituents. The 1<sup>st</sup>, 2<sup>nd</sup>, 3<sup>rd</sup> and 4<sup>th</sup> functions introduced are shown in blue, green, brown and pink, respectively.

## Results and discussion

### Synthesis

In order to completely decorate the ferrocene scaffold with different substituents, our idea was to identify a substrate both 1,1'-disubstituted with chiral DGs and easy to access. (*R,R*)-*S,S'*-Di-*tert*-butylferrocene-1,1'-disulfoxide (**1**) fulfilled our requirements as it has already been tested in deprotonation-trapping by Zhang's team.<sup>86</sup> However, we did not use their approach in two steps towards **1** (conversion of ferrocene to 1,1'-di(*tert*-butylthio)ferrocene followed by Kagan's asymmetric oxidation; 30% yield from 1,1'-dilithioferrocene), and preferred a one pot procedure. Thus, the disulfoxide **1** was easily prepared in 41% yield by reacting ferrocene-1,1'-dilithium<sup>87</sup> with (*R*)-*S*-*tert*-butyl-*tert*-butanethiosulfinate<sup>88</sup> (Scheme 1, top).

While Zhang and co-workers employed *n*-butyllithium in tetrahydrofuran (THF) at 0 °C to deprotonate the disulfoxide **1**,<sup>86</sup> we instead used *tert*-butyllithium at –80 °C. Under these conditions, the derivatives **R<sub>p</sub>R<sub>p</sub>-2** were isolated after electrophilic trapping with deuterated water (product **2a**), dimethylformamide (**2b**), benzophenone (**2c**), *N*-fluorobenzenesulfonimide (NFSI; **2d**), diphenyl disulfide (**2e**) and chlorotrimethylsilane (**2f**). With NFSI as the electrophile, better yield (79%) and reproducibility were achieved by working at –90 °C with 3 equivalents of *tert*-butyllithium (Scheme 1, middle). When dichlorodimethylsilane was used, the expected bridged silane<sup>89</sup> was not obtained and we rather isolated the two siloxanes<sup>84</sup> **2g1** and **2g2**, as well as the bis-silanol **2g3** (Scheme 1, bottom). While the formation of **2g1** and **2g3** probably originates from the hydrolysis of an inter-



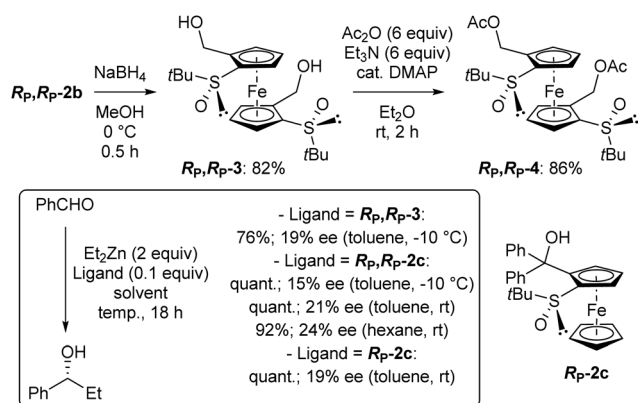
Scheme 1 Synthesis of the 2,2'-disubstituted (*R,R*)-*S,S'*-di-*tert*-butylferrocene-1,1'-disulfoxides **R<sub>p</sub>R<sub>p</sub>-2** from ferrocene. <sup>a</sup> Electrophiles used: D<sub>2</sub>O (**2a**), Me<sub>2</sub>NCHO (**2b**), Ph<sub>2</sub>C=O (**2c**), (PhSO<sub>2</sub>)<sub>2</sub>NF (**2d**), PhSSPh (**2e**), ClSiMe<sub>3</sub> (**2f**) and Cl<sub>2</sub>SiMe<sub>2</sub> (**2g**). <sup>b</sup> After hydrolysis. <sup>c</sup> Reaction performed at –90 °C. <sup>d</sup> Monofluoride also isolated by reducing the amount of base to 2.5 equivalents (see ESI†).



mediate 2,2'-bis(chlorodimethylsilyl)ferrocene-1,1'-disulfoxide, it is currently more difficult to explain the formation of the higher siloxane **2g2**. However, this surprising result prompted us to take a closer look at the reactivity of these ferrocene-1,1'-disulfoxides.

One application of chiral arylmethanols is their use as ligands in the addition of diethylzinc to benzaldehyde.<sup>90–94</sup> This reaction was considered here to evaluate the catalytic potential of the compound **R<sub>P</sub>,R<sub>P</sub>-2c**, which is close to the C<sub>2</sub>-symmetric ligand of Ikeda and co-workers.<sup>95</sup> For comparison purposes, we also prepared the diol **R<sub>P</sub>,R<sub>P</sub>-3**, lacking the *gem*-diphenyl moiety, by reduction of **R<sub>P</sub>,R<sub>P</sub>-2b** (Scheme 2, top left). When benzaldehyde was treated with diethylzinc in toluene containing a catalytic amount of **R<sub>P</sub>,R<sub>P</sub>-3** at –10 °C overnight,<sup>95</sup> the expected alcohol was isolated in 76% yield and 19% ee in favour of the *R* enantiomer (Scheme 2, bottom). Under the same reaction conditions, the diol **R<sub>P</sub>,R<sub>P</sub>-2c** afforded the product in quantitative yield and an ee of 15%, while working at room temperature led to a 21% ee. Finally, replacing toluene with hexane<sup>94</sup> gave an almost similar result (92% yield, 24% ee). For comparison, we finally used the 1,2-disubstituted ferrocene **R<sub>P</sub>-2c** (see ESI†) in toluene at rt and obtained the alcohol with similar yield and ee. A similar trend for di- vs. tetra-topic ligands has been previously reported,<sup>95</sup> although here with lower enantioselectivity.

The diacetate **R<sub>P</sub>,R<sub>P</sub>-4** also appeared to us as a suitable substrate to attempt the synthesis of the corresponding 2-phospha[3]ferrocenophanes. Indeed, related ferrocene-based chiral phosphines have been successfully used as organocatalysts for enantioselective transformations.<sup>96–98</sup> This diacetate was easily prepared from the diol **R<sub>P</sub>,R<sub>P</sub>-3** (Scheme 2, top right). However, whether from the diol **R<sub>P</sub>,R<sub>P</sub>-3** or the diacetate **R<sub>P</sub>,R<sub>P</sub>-4**, no substitution occurred with phosphino<sup>99</sup> or (phosphinomethyl)ferrocene<sup>100</sup> in acetic acid at room<sup>101</sup> or at reflux<sup>96</sup> temperature. Inspired by a previous study carried out in our group,<sup>102</sup> we also attempted to replace the two acetates with these phosphines (as well as amines and diamines; see ESI†) in hexafluoroisopropanol at 60 °C, but without success. The recovery of the starting material in all these reactions shows the very



**Scheme 2** Attempts to use the alcohols **R<sub>P</sub>,R<sub>P</sub>-3**, **R<sub>P</sub>,R<sub>P</sub>-2c** and **R<sub>P</sub>-2c** as ligands in the diethylzinc addition to benzaldehyde.

low reactivity of this sterically hindered diacetate in substitution reactions. On the other hand, the particular behaviour of these 1,1',2,2'-tetrasubstituted ferrocenes can also be seen as an opportunity to study original reactivities.

We next explored the possibility to reach more substituted derivatives from the 1,1',2,2'-tetrasubstituted ferrocenes **R<sub>P</sub>,R<sub>P</sub>-2e** and **R<sub>P</sub>,R<sub>P</sub>-2f**. Indeed, their 1,2-disubstituted counterparts **R<sub>P</sub>-2e** and **R<sub>P</sub>-2f** (see Fig. 3a and b) can be functionalized at the remaining position next to the sulfoxide by deprotonation in THF either with an excess of *n*-butyllithium at room temperature<sup>84</sup> or with *tert*-butyllithium at –80 °C.<sup>85</sup> Therefore, we tried to introduce two additional substituents from **R<sub>P</sub>,R<sub>P</sub>-2e** and **R<sub>P</sub>,R<sub>P</sub>-2f** in a similar way. For this purpose, **R<sub>P</sub>,R<sub>P</sub>-2e** was first treated with *tert*-butyllithium (3 equiv.) at –80 °C for 1 h before trapping with chlorotrimethylsilane. Surprisingly, the 4,4'-disilylated product **R<sub>P</sub>,R<sub>P</sub>-5a** was obtained in 40% yield instead of the expected 5,5'-disilylated derivative, as well as the 4-monosilylated derivative **R<sub>P</sub>,R<sub>P</sub>-5'a** in 11% yield (Scheme 3).

In 2015, structurally-related 1,1',2,2',4,4'-hexasubstituted ferrocenes were synthesized by Pirió, Hierso and co-workers by double deprotonation of *dl*-1,1'-bis[(dialkylamino)methyl]-3,3'-di-*tert*-butylferrocenes.<sup>103</sup> However, in our case, we bene-

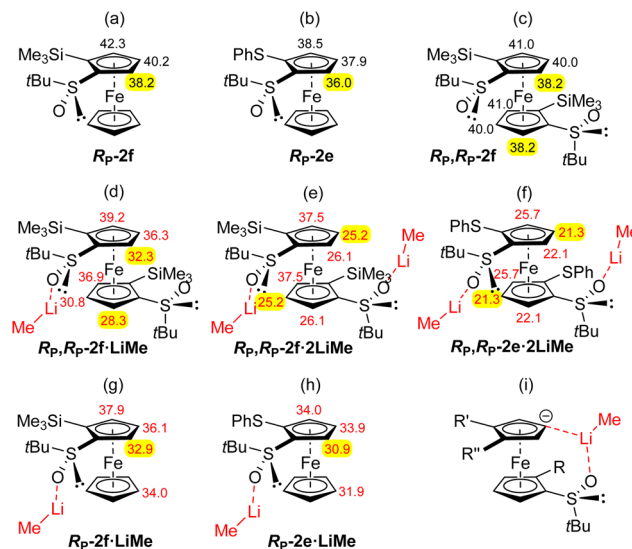
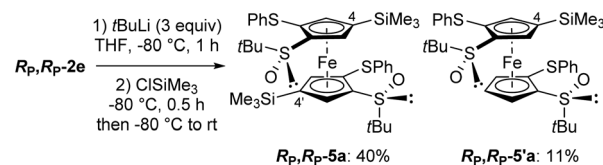


**Fig. 3** Top. Selected calculated pK<sub>a</sub> values of **R<sub>P</sub>-2f** (a), **R<sub>P</sub>-2e** (b) and **R<sub>P</sub>,R<sub>P</sub>-2f** (c). Middle. pK<sub>a</sub> values of **R<sub>P</sub>,R<sub>P</sub>-2f** (d), **R<sub>P</sub>,R<sub>P</sub>-2f** (e) and **R<sub>P</sub>,R<sub>P</sub>-2e** (f) as complexes with one, two and two LiMe, respectively. Bottom. pK<sub>a</sub> values of **R<sub>P</sub>-2f** (g) and **R<sub>P</sub>-2e** (h) as complexes with one LiMe, and a schematic of the stabilization effect (i).



**Scheme 3** Deprotonation-trimethylsilylation of (*R,R*,*R<sub>P</sub>,R<sub>P</sub>*)-*S,S'*-di-*tert*-butyl-2,2'-di(phenylthio)ferrocene-1,1'-disulfoxide (**R<sub>P</sub>,R<sub>P</sub>-2e**).



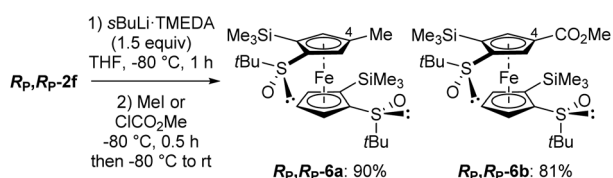
fitted from the presence of the chiral sulfoxides to reach enantiopure 1,1',2,2',4,4'-hexasubstituted ferrocenes by double deprotolithiation-trapping.

To favour the formation of a dilithiated intermediate, the reaction was also performed at higher temperature ( $-50\text{ }^{\circ}\text{C}$ ). However, degradation mainly occurred (the 4,4'-diiodinated derivative  $R_p,R_p\text{-}5b$  was only isolated in 14% yield after iodolysis; see ESI†). This tends to suggest that the lithiated intermediates easily undergo decomposition, especially if they are not quickly trapped with an electrophile.

We were keen to see if this deprotometallation remote from the directing group could be extended to other substrates, and therefore selected  $R_p,R_p\text{-}2f$  in which the phenylthio groups of  $R_p,R_p\text{-}2e$  are replaced with trimethylsilyls. Pleasingly, the use of TMEDA-activated *sec*-butyllithium (TMEDA = *N,N,N',N'*-tetramethylethylenediamine; 1.5 equiv.) in THF at  $-80\text{ }^{\circ}\text{C}$  for 1 h allowed the ferrocene 4-position of  $R_p,R_p\text{-}2f$  to be cleanly deprotolithiated, as demonstrated by subsequent trapping with iodomethane and methyl chloroformate, leading to the products  $R_p,R_p\text{-}6a$  (90% yield) and  $R_p,R_p\text{-}6b$  (81% yield), respectively (Scheme 4). Note that trapping with concentrated DCl furnished, in addition to the expected 4-deuterated derivative (70%), the 5-deuterated one, next to the sulfoxide (20%). This confirms the presence of a major, although not exclusive, 4-lithiated derivative before the trapping step. This result is also consistent with the equilibrium constant calculated in this work for the transformation of an anion at C5 into an anion at C4, both coordinated with two LiMe (Fig. 3e), which is approximately equal to 8.

However, all attempts to introduce a sixth substituent from the 4-methyl-2,2'-bis(trimethylsilyl)ferrocene-1,1'-disulfoxide  $R_p,R_p\text{-}6a$  by using *sec*-butyllithium-TMEDA and subsequent trapping failed with either Eschenmoser's salt, chlorotrimethylsilane or chlorodiphenylphosphine as the electrophile. In addition, under similar reaction conditions,  $R_p,R_p\text{-}6b$  was only moderately converted ( $\sim 25\%$ ) into the 4,4'-disubstituted product  $R_p,R_p\text{-}6'b$  (see ESI†) after trapping with methyl chloroformate. Therefore, we came to the conclusion that, to reach 1,1',2,2',4,4'-hexasubstituted derivatives, it would be preferable to start from  $R_p,R_p\text{-}2f$  and perform a double deprotolithiation-trapping sequence.

Preliminary tests were performed by using either *tert*-butyllithium (2.6 equiv.) at  $-80$  or  $-50\text{ }^{\circ}\text{C}$ , or *n*-butyllithium (3 equiv.) at  $0\text{ }^{\circ}\text{C}$ , in THF. However, after interception with iodine, mixtures of 4-mono and polyiodinated products as well

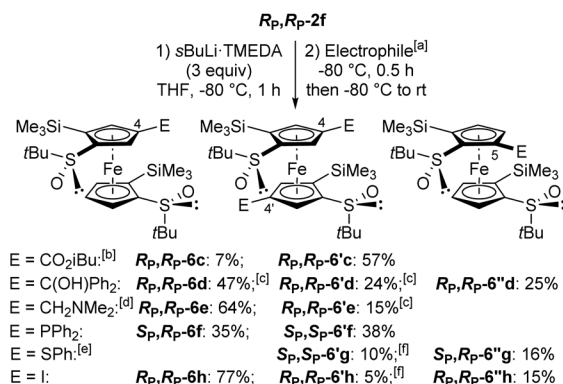


**Scheme 4** Deprotometallation-trapping of (*R,R,R<sub>p</sub>,R<sub>p</sub>*)-*S,S'*-di-*tert*-butyl-2,2'-bis(trimethylsilyl)ferrocene-1,1'-disulfoxide ( $R_p,R_p\text{-}2f$ ) using *sec*-butyllithium-TMEDA (1.5 equiv.).

as starting material were obtained. Further, attempts to deprotometallate  $R_p,R_p\text{-}2f$  using lithium 2,2,6,6-tetramethylpiperidide (LiTMP; 6 or 12 equiv.) in the presence of ZnCl<sub>2</sub>·TMEDA (2 or 4 equiv.) as an *in situ* trap provided only inseparable mixtures of the starting material and its 4-iodinated derivative (see ESI†).

Since the 4,4'-difunctionalized product  $R_p,R_p\text{-}6'c$  was already present (21% yield) in a test reaction using the *sec*-butyllithium-TMEDA chelate (1.5 equiv.) in THF at  $-80\text{ }^{\circ}\text{C}$  for 1 h and isobutyl chloroformate as the electrophile (see ESI†), we decided to increase the amount of this base to access enantiopure 1,1',2,2',4,4'-hexasubstituted ferrocenes (Scheme 5). Thus, by using *sec*-butyllithium-TMEDA (3 equiv.), the expected product  $R_p,R_p\text{-}6'c$  was obtained in 57% yield while the 4-functionalized product  $R_p,R_p\text{-}6c$  was isolated in only 7% yield. In contrast, with benzophenone as the electrophile, the only pure product isolated, in 25% yield, was the 5-substituted product  $R_p,R_p\text{-}6''d$ , from a crude also containing the 4-substituted  $R_p,R_p\text{-}6d$  ( $\sim 47\%$  yield) and the 4,4'-disubstituted ( $\sim 24\%$  yield)  $R_p,R_p\text{-}6'd$  derivatives. Moreover, the use of Eschenmoser's salt provided the corresponding 4-(dimethylaminomethylated) ferrocene-1,1'-disulfoxide  $R_p,R_p\text{-}6e$  as the main product (64% yield). With chlorodiphenylphosphine, the mono and diphosphines  $S_p,R_p\text{-}6f$  and  $S_p,S_p\text{-}6'f$  were isolated with yields of 35% and 38%, respectively. However, when diphenyl disulfide was employed, the corresponding di and monofunctionalized products  $S_p,R_p\text{-}6'g$  and  $S_p,S_p\text{-}6''g$  were formed in low yields, 10% and 16% respectively, due to recovery of 59% of the starting material. Finally, the use of iodine led to the 4-monoiodinated product  $R_p,R_p\text{-}6h$  as the main product (77% yield) beside the corresponding product  $R_p,R_p\text{-}6''h$  (15% yield).

Our results concerning the functionalization of  $R_p,R_p\text{-}2e$  and  $R_p,R_p\text{-}2f$  contrast with those of Park and co-workers who converted *C*<sub>2</sub>-symmetric 1,1'-bis(diphenylphosphino)-2,2'-di(4-



**Scheme 5** Deprotometallation-trapping of (*R,R,R<sub>p</sub>,R<sub>p</sub>*)-*S,S'*-di-*tert*-butyl-2,2'-bis(trimethylsilyl)ferrocene-1,1'-disulfoxide ( $R_p,R_p\text{-}2f$ ) using *sec*-butyllithium-TMEDA (3 equiv.). <sup>a</sup> Electrophiles used: ClCO<sub>2</sub>iBu (**6c/6'c**), Ph<sub>2</sub>C=O (**6d/6'd/6''d**), CH<sub>2</sub>=NMe<sub>2</sub> (**6e/6'e**), ClPPh<sub>2</sub> (**6f/6'f**), PhSSPh (**6'g/6''g**) and I<sub>2</sub> (**6h/6'h/6''h**). <sup>b</sup> Recovery of 2% of the starting material. <sup>c</sup> Estimated yield. <sup>d</sup> Recovery of 18% of the starting material. <sup>e</sup> Recovery of 59% of the starting material. <sup>f</sup> Yield given after cleavage of the trimethylsilyl groups.



isopropyl-2-oxazolyl)ferrocene to the stereopure 3,3'-disilylated derivative using a similar deprotolithiation-trapping sequence ( $s\text{BuLi}\cdot\text{ClSiMe}_3$ ).<sup>104</sup> A more related study was reported by Brown and co-workers who claimed the deprotonation at C3 of (*tert*-butylthio)ferrocene using *sec*-butyllithium in THF.<sup>105,106</sup> However, no detailed explanation was provided for this result. In order to compare the stabilities of the 4- and 5-lithiated derivatives of  $R_P,R_P\text{-}2e$  and  $R_P,R_P\text{-}2f$ , the equilibrium CH acidities of different positions were determined. The  $pK_a$  values, calculated as before within the DFT framework (see ESI† for details),<sup>107–110</sup> are presented in Fig. 3.

We have previously noticed that for mono and disubstituted ferrocenes with markedly distinct acidities at different positions,<sup>108,109</sup> the  $pK_a$  values are good indicators for deprotolithiation-trapping sequences. But when acidities are close and bulky substituents present,<sup>85,107</sup> coordination to lithium should further be considered. Compared to the values previously obtained for  $R_P\text{-}2f$ ,<sup>85</sup> those of  $R_P,R_P\text{-}2f$  are quite similar (Fig. 3c) and do not differ significantly within the molecule. As coordination to lithium significantly impacts deprotolithiations, *e.g.* through stabilization of transition states and lithiated products by formation of cyclic structures involving a lithium ion,<sup>85,111</sup>  $pK_a$  values were also calculated for the complexes  $R_P,R_P\text{-}2f\text{-LiMe}$  (Fig. 3d),  $R_P,R_P\text{-}2f\text{-}2\text{LiMe}$  (Fig. 3e) and  $R_P,R_P\text{-}2e\text{-}2\text{LiMe}$  (Fig. 3f). To this end, the various alkyllithiums used in the experiments were replaced by methylolithium in the calculations.

These data allow some comments on the regioselectivity observed in these deprotometallations. Indeed, for the 1,2-disubstituted ferrocenes  $R_P\text{-}2f$  and  $R_P\text{-}2e$ , coordination of the oxygen of the sulfinyl group to lithium lowers the  $pK_a$  values by up to  $\sim 5$  units (Fig. 3g and h). According to the calculations, the position next to the sulfoxide remains the most acidic, in line with the observed regioselectivity during the functionalization of  $R_P\text{-}2f$ .<sup>86</sup> In contrast, the  $pK_a$  values of  $R_P,R_P\text{-}2f\text{-LiMe}$ ,  $R_P,R_P\text{-}2f\text{-}2\text{LiMe}$  and  $R_P,R_P\text{-}2e\text{-}2\text{LiMe}$  (Fig. 3d–f) tend to suggest that a ferrocenyl anion formed by deprotonation can be significantly stabilized by a remote sulfoxide through coordination to lithium. In this scenario, the stabilization probably results from the formation of a bridged structure involving a lithium ion such as the one depicted in Fig. 3i. Furthermore, one should keep in mind the small energy barrier separating the staggered and eclipsed conformations of the cyclopentadienyl rings (usually of the order of thermal energy).<sup>112</sup> This could explain why the above mentioned stabilization is possible under deprotonation in both positions 4 and 5 (Fig. 3e and f). Furthermore, the  $pK_a$  values of  $R_P,R_P\text{-}2f\text{-}2\text{LiMe}$  and  $R_P,R_P\text{-}2e\text{-}2\text{LiMe}$  (putative species, as the base is used in excess), tend to show that the 4-lithiated derivatives are slightly more stable than the 5-lithiated ones, in good agreement with our experimental results (Schemes 3–5). Finally, for the ferrocene  $R_P,R_P\text{-}2e$  the abovementioned stabilization (see ESI† for illustration) is possible under deprotonation in all three positions of the remote cyclopentadienyl ring while for the bulkier ferrocene  $R_P,R_P\text{-}2f$  in positions 4 and 5 only (Fig. 3e and f).

Since deprotometallations using alkyllithiums are generally not reversible, the most stable ferrocenyllithiums are not always produced, and conformations can also play a role. Indeed, in their related study on the double deprotometallation of 1,1'-bis(trimethylsilyl)ferrocene, Roberts, Silver and co-workers attributed the selective formation of a  $C_2$ -symmetric diastereomer to the smaller steric interactions between the silyl groups in the dilithiated intermediate.<sup>113,114</sup> Similarly, one could imagine that the ferrocene  $R_P,R_P\text{-}2f$  adopts a privileged conformation in which the trimethylsilyl groups move away from each other to limit the steric hindrance (conformation found in the solid state and in solution in  $\text{CDCl}_3$ ; see below and ESI†). Thus, the regioselectivity observed could also correspond to the least sterically hindered deprotolithiation position.

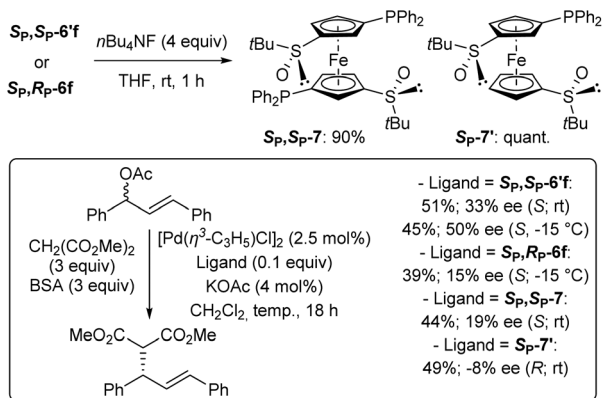
However, some discrepancies between the results obtained with different electrophiles from  $R_P,R_P\text{-}2f$  using 3 equivalents of base (Scheme 5) remain difficult to interpret. The main question that arises is whether a dilithiated intermediate is formed before the addition of the electrophile or whether the generated 4-functionalized product undergoes a second deprotometallation-trapping sequence.

We already observed that the conversion of a 1,1',2,2',4-penta into a 1,1',2,2',4,4'-hexasubstituted ferrocene was hardly possible. Indeed, the deprotometallation of the methyl ester  $R_P,R_P\text{-}6b$  using *sec*-butyllithium·TMEDA before interception with methyl chloroformate only afforded 17% of  $R_P,R_P\text{-}6'b$ . However, when similar deprotometallation conditions were applied to the isobutyl ester  $R_P,R_P\text{-}6c$  before adding isobutyl chloroformate as the electrophile, the expected product  $R_P,R_P\text{-}6'c$  was not observed. Thus, even if it cannot be totally excluded in the case of electrophiles enough compatible with hindered alkyllithiums (*e.g.* chlorotrimethylsilane), all these data make an *in situ* deprotometallation-trapping sequence from the 4-functionalized product formed rather unlikely. Consequently, what seems most reasonable is that after its reaction with a first equivalent of electrophile, the 4,4'-dilithiated intermediate finds itself in a situation where it is more or less able (depending on the steric hindrance generated or/and the reactivity of the electrophile) to attack the second equivalent of electrophile before hydrolysis happens. For example, steric hindrance might be too high in the case of benzophenone or iodine while reactivity might be too low in the case of Eschenmoser's salt.

As some of the 4,4'-substituted ferrocenes prepared so far might behave as ligands, we were eager to evaluate them in asymmetric catalysis. Therefore, inspired by studies of Snieckus and co-workers who successfully used the enantiopure  $C_2$ -symmetric *N,N*-diisopropyl-2,2'-bis(diphenylphosphino)ferrocene-1,1'-dicarboxamide as ligand for enantioselective palladium-catalysed allylic substitution,<sup>115</sup> we selected for this purpose the di and monophosphines  $S_P,S_P\text{-}6'f$  and  $S_P,R_P\text{-}6'f$ , as well as the corresponding desilylated counterparts  $S_P,S_P\text{-}7$  and  $S_P\text{-}7'$  (Scheme 6, top).

They were involved in the reaction of racemic (*E*)-1,3-diphenyl-2-propenyl acetate with dimethyl malonate (3 equiv.) under





**Scheme 6** Attempts to use the phosphines  $\text{Sp},\text{Sp}-6'\text{f}$ ,  $\text{Sp},\text{Rp}-6\text{f}$ ,  $\text{Sp},\text{Sp}-7$  and  $\text{Sp}-7'$  as ligands in the palladium-catalysed allylic substitution of racemic phenylcinnamyl acetate with dimethyl malonate.

Trost conditions using catalytic allylpalladium(II) chloride dimer, ligand and potassium acetate, and excess of *N,O*-bis-(trimethylsilyl)acetamide (BSA) in dichloromethane at room temperature.<sup>116</sup> Under these conditions, the best ligand proved to be the diphosphine  $\text{Sp},\text{Sp}-6'\text{f}$ , giving the expected product in 45% and a moderate enantioselectivity (50% ee) in favour of the *S* enantiomer (Scheme 6, bottom).

The results obtained so far (Scheme 5 and Fig. 3e) suggest that the steric hindrance generated by the two trimethylsilyl groups of the substrate  $\text{Rp},\text{Rp}-2\text{f}$  interferes with the synthesis of a deca-substituted ferrocene. Hence, we decided to continue with the less crowded 2,2'-difluorinated ferrocene  $\text{Rp},\text{Rp}-2\text{d}$  for which the  $\text{p}K_{\text{a}}$  values are also promising for further functionalization, expected next to fluorine (Fig. 4).

We first tested the double functionalization of  $\text{Rp},\text{Rp}-2\text{d}$  by using LiTMP (2.5 equiv.) in the presence of TMEDA (1.4 equiv.) in hexane at rt for 20 min, as proposed by Butler for the double deprotonation of polyhalogenated ferrocenes.<sup>117</sup> However, only starting material and degradation products were observed under these conditions. Next, we switched to *sec*-butyllithium in THF at -80 °C for 1 h, as used for fluoroferrocene.<sup>108</sup> After subsequent quenching with chlorotrimethylsilane, the expected disilylated product  $\text{Rp},\text{Rp}-2\text{a}$  was obtained in an encouraging 38% yield although degradation was also observed at this temperature. At -90 °C, the use of *sec*-butyllithium·TMEDA (3 equiv.) led to a slightly improved 44% yield. In order to progress towards more substituted derivatives, we then successively treated  $\text{Rp},\text{Rp}-2\text{d}$  with *sec*-butyllithium (3 equiv.) and hexachloroethane, leading to the 3,3'-dichlorinated derivative  $\text{Sp},\text{Sp}-8\text{b}$  in 61% yield. Finally, we simi-

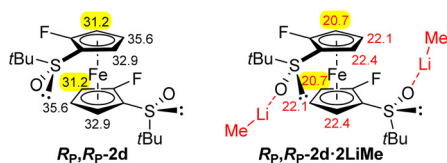
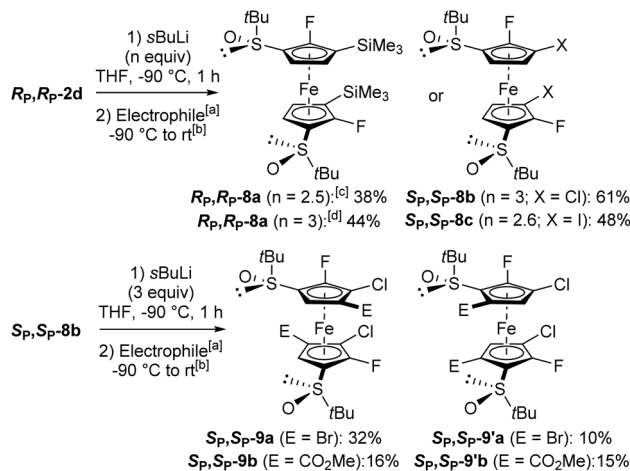


**Fig. 4**  $\text{p}K_{\text{a}}$  values of  $\text{Rp},\text{Rp}-2\text{d}$  and its complex with two  $\text{LiMe}$ .



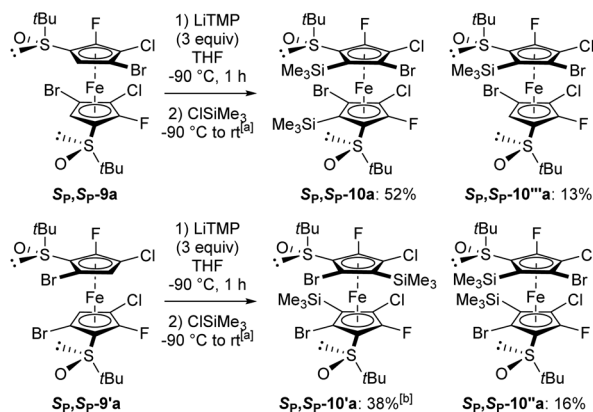
**Scheme 7** Synthesis of hexa and octasubstituted ferrocenes. <sup>a</sup> Electrophiles used:  $\text{ClSiMe}_3$  ( $\text{Rp},\text{Rp}-8\text{a}$ ),  $\text{C}_2\text{Cl}_6$  ( $\text{Sp},\text{Sp}-8\text{b}$ ),  $\text{I}_2$  ( $\text{Sp},\text{Sp}-8\text{c}$ ),  $\text{CF}_3\text{CFBrCF}_2\text{Br}$  ( $\text{Sp},\text{Sp}-9\text{a}$  and  $\text{Sp},\text{Sp}-9\text{a}'$ ), and  $\text{ClCO}_2\text{Me}$  ( $\text{Sp},\text{Sp}-9\text{b}$  and  $\text{Sp},\text{Sp}-9\text{b}'$ ). <sup>b</sup> See ESI† for details on the trapping step. <sup>c</sup> -80 °C instead of -90 °C. <sup>d</sup> In the presence of TMEDA (3 equiv.).

larly prepared the corresponding diiodide  $\text{Sp},\text{Sp}-8\text{c}$  in 48% yield (Scheme 7, top). We attempted to isomerize this iodide by heavy halogen migration<sup>22,74</sup> using LiTMP (3.4 equiv.) under the conditions described previously (THF, -50 °C, 2 h).<sup>107</sup> However, after hydrolysis, deiodinated product was mainly formed (29% yield), resulting from a competitive iodine/lithium exchange.<sup>107,108,118,119</sup> The expected 2,2'-difluoro-4,4'-diiodoferrocene-1,1'-disulfoxide was only detected in one of the fractions separated by column chromatography (12% estimated yield).

In order to progress towards unprecedented octasubstituted ferrocene disulfoxides, we treated the 3,3'-dichlorinated derivative  $\text{Sp},\text{Sp}-8\text{b}$  with *sec*-butyllithium (2.6 equiv.) in THF at -90 °C for 1 h. As subsequent deuteration led to a mixture of regioisomers, we attempted to use other electrophiles. By trapping with 1,2-dibromo-1,1,2,3,3,3-hexafluoropropane, two octasubstituted ferrocenes were isolated:  $\text{Sp},\text{Sp}-9\text{a}$  possessing its bromine atoms next to the chlorines (32% yield), and its regioisomer  $\text{Sp},\text{Sp}-9\text{a}'$  with its bromine atoms next to the sulfoxides (10% yield). Similarly, the use of methyl chloroformate afforded the two regioisomers  $\text{Sp},\text{Sp}-9\text{b}$  and  $\text{Sp},\text{Sp}-9\text{b}'$ , respectively possessing their ester functions next to the chlorines (16% yield) and next to the sulfoxides (15% yield; Scheme 7, bottom). Although the functionalization of the 5 and 5' positions was not expected from the substrate **8b**, a similar reaction was recently observed on related ferrocenesulfoxides.<sup>85</sup>

To finally reach deca-substituted ferrocenes, the regioisomers  $\text{Sp},\text{Sp}-9\text{a}$  and  $\text{Sp},\text{Sp}-9\text{a}'$  were subjected to the action of an excess of LiTMP (3 equiv., -90 °C, 1 h) before trapping with chlorotrimethylsilane. From  $\text{Sp},\text{Sp}-9\text{a}$ , this made it possible to isolate the deca-substituted derivative  $\text{Sp},\text{Sp}-10\text{a}$  as the main product (52% yield; Scheme 8, top). The use of methyl chloroformate for the trapping step also led to the corresponding product  $\text{Sp},\text{Sp}-10\text{b}$ , but in a lower 10% yield (see ESI†). By start-





**Scheme 8** Synthesis of nona and decasubstituted ferrocenes. <sup>a</sup> See ESI† for details on the trapping step. <sup>b</sup> (*R,R,S\_p,S\_p*)-2,5'-dibromo-*S,S'*-di-*tert*-butyl-4,3'-dichloro-5,2'-difluoro-3-(trimethylsilyl)ferrocene-1,1'-disulfoxide (*S\_p,S\_p*-10''*a*) was also isolated in 14% yield.

ing from *S\_p,S\_p*-9'*a*, the disilylated *S\_p,S\_p*-10'*a* coming from a double deprotonation-trapping sequence was also obtained as the main product (38% yield); however, it was accompanied by the regioisomer *S\_p,S\_p*-10''*a* (16% yield; Scheme 8, bottom). For the latter, a single halogen migration took place on one cyclopentadienyl (Cp) ring before trapping. Single deprotonation also took place in these two reactions, leading to the nonasubstituted ferrocenes *S\_p,S\_p*-10''*a* (13% yield; Scheme 8, top) and *S\_p,S\_p*-10''''*a* (14% yield).

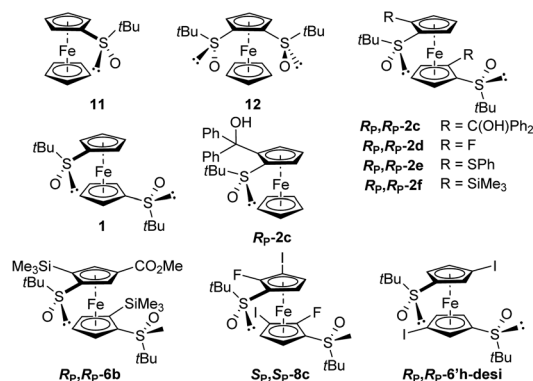
Thus, the first enantiopure hexa, octa, nona and decasubstituted ferrocenes could be achieved for the first time. Although none of these highly substituted ferrocenes afforded crystals suitable for X-ray diffraction analysis, high-resolution mass spectrometry analysis as well as the comparison of the NMR spectra (in particular, the <sup>1</sup>H, <sup>13</sup>C, NOESY and HOESY data) supported the proposed structures.

### Electrochemical characterization

Few studies have been dedicated to the evaluation of the electrochemical behaviour of ferrocene sulfoxides. In 1997, Kagan highlighted the electron-withdrawing properties of the sulfoxide group as various alkyl- and aryl-sulfoxides raise the redox potentials from +0.25 to +0.29 V vs. FcH/FcH<sup>+</sup>.<sup>120</sup> Except for *S*-butylferrocenesulfoxide, the *E*<sub>1/2</sub> values of the *S*-arylated ferrocenesulfoxides were slightly higher than those of the *S*-alkylated ones. More recently, Jahn reported that the introduction of a phenylsulfinyl raises the redox potential of ferrocene by +0.30 V vs. FcH/FcH<sup>+</sup>,<sup>51</sup> close to the +0.28 V value reported by Kagan. However, the introduction of a phenylsulfinyl group on each Cp ring raises the *E*<sub>1/2</sub> value by only +0.50 V vs. FcH/FcH<sup>+</sup>. Taking advantage of the various ferrocene-1,1'-disulfoxides described in this study, we were eager to further investigate the electrochemical properties of these derivatives. This was done by performing cyclic voltammetry (CV) and differential pulse voltammetry (DPV) analyses in dry, oxygen-free dichloromethane (Table 1).

**Table 1** Electrochemical data (in V) for selected ferrocene sulfoxides<sup>a</sup>

Compound	<i>E</i> <sub>pa</sub> <sup>b</sup>	<i>E</i> <sub>pc</sub> <sup>b</sup>	<i>i</i> <sub>pa</sub> / <i>i</i> <sub>pc</sub> <sup>b</sup>	<i>E</i> <sub>1/2</sub> <sup>c</sup>
<b>11</b>	0.29	0.19	1.0	0.22
<b>12</b>	0.49	0.40	0.80	0.38
<b>1</b>	0.49	0.40	0.92	0.44
<i>R_p,R_p</i> -2c	0.36	0.27	1.0	0.32
<i>R_p,R_p</i> -2c	0.68	0.59	0.90	0.61
<i>R_p,R_p</i> -2d	0.74	nd <sup>d</sup>	nd <sup>d</sup>	0.63
<i>R_p,R_p</i> -2e	0.38	0.29	1.0	0.33
<i>R_p,R_p</i> -2f	0.47	0.37	1.0	0.42
<i>R_p,R_p</i> -6b	0.68	0.58	1.0	0.60
<i>S_p,S_p</i> -8c	0.87	nd	nd	0.79
<i>R_p,R_p</i> -6'h-desi	0.77	0.70	1.0	0.71



<sup>a</sup> Potential values referenced to Ag/AgCl and recalculated to FcH/FcH<sup>+</sup>; scan rate = 100 mV s<sup>-1</sup>. <sup>b</sup> From CV experiments. <sup>c</sup> From DPV experiments. <sup>d</sup> Not determined due to irreversible oxidation.

For comparison purposes, we also included (*R,R*)-*S*-*tert*-butyl-2-[( $\alpha,\alpha$ -diphenyl)hydroxymethyl]ferrocenesulfoxide (*R\_p,R\_p*-2c), and the previously reported (*S*)-*S*-*tert*-butylferrocenesulfoxide (**11**) and (*R,R*)-*S,S'*-di-*tert*-butylferrocene-1,2-disulfoxide (**12**).

The introduction of a phenylsulfinyl onto ferrocene raised the redox potential by +0.22 V, close to the +0.25 V value recorded by Kagan in different analysis conditions. The introduction of a second sulfoxide group further increases the *E*<sub>1/2</sub> value from +0.18 to +0.22 V, depending on the position functionalized. Indeed, it seems that when introduced next to the first sulfoxide, the second one cannot exert its full effect (compound **12**). However, when introduced on the other Cp ring (compound **1**; Fig. 5), a fully additive effect was noticed which perfectly matched with the  $\sum\sigma_p$  Hammett parameters (*E*<sub>1/2</sub> = 2.227  $\sum\sigma_p$  - 0.0215, *R*<sup>2</sup> = 1, Plot ESI†). Similar results were previously reported by others who plotted the *E*<sub>1/2</sub> value against the sum of different Hammett parameters, depending on the substituent studied.<sup>53,121–125</sup> From the compound **11**, the introduction of a tertiary alcohol raised the redox potential by +0.10 V with the compound *R\_p,R\_p*-2c while the introduction of two alcohol groups from the ferrocene **1** only raised the redox potential by +0.17 V (compound *R\_p,R\_p*-2c). This additivity trend was confirmed with the difluorinated compound *R\_p,R\_p*-2d (+0.10 V per fluorine atom) although an irreversible oxidation was also observed. However, while the trimethylsilyl group had almost no effect (compound *R\_p,R\_p*-2f), the introduction of two phenylthio substituents lowered the *E*<sub>1/2</sub> value by



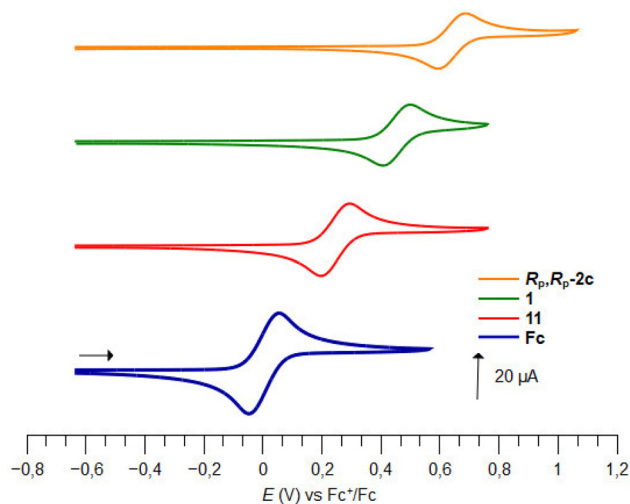


Fig. 5 Plots of cyclic voltammograms of ferrocene (Fc) and the derivatives **11**, **1** and **R<sub>p</sub>R<sub>p</sub>-2c**.

−0.11 V, a surprising result considering the increase of  $E_{1/2}$  by +0.13 V per phenylthio substituent already observed.<sup>41,51</sup> From the tetrasubstituted ferrocene **R<sub>p</sub>R<sub>p</sub>-2d**, the introduction of two iodine atoms next to the fluorine raised the redox potential by +0.08 V per iodine. However, when the iodine atoms were introduced remoted from another group (compound **R<sub>p</sub>R<sub>p</sub>-6'h-desi**), the redox potential increased by +0.13 V per iodine, in better agreement with the +0.15 V expected value.<sup>124</sup> From the tetrasubstituted ferrocene **R<sub>p</sub>R<sub>p</sub>-2f** to the pentasubstituted compound **R<sub>p</sub>R<sub>p</sub>-6b**, an increase of +0.18 V was recorded, which is lower than the expected value (+0.22 V from the work of Jahn,<sup>51</sup> +0.26 V from the work of Heinze<sup>53</sup>).

Therefore, taking together, these results tend to highlight the importance of the substituent, and its position, already present on a ferrocene derivative on the redox potential. To get a more general view on the substituent effect in this ferrocene-1,1'-disulfoxide series, we plotted the  $E_{1/2}$  values of ferrocene and the compounds **1**, **2c**, **2d**, **2f**, **8c** and **R<sub>p</sub>R<sub>p</sub>-6'h-desi** against either the sums of  $\sigma_p$ ,  $\sigma_m$  or  $\sigma_p + \sigma_m$  (plots ESI2–4†). Given the diversity of substituents, the best correlation was obtained with the equation  $E_{1/2} = 1.751 \sum\sigma_p + 0.048$ ,  $R^2 = 0.9438$ . However, focusing our study on the effect of halogen atoms resulted in a better correlation between the redox potential value and the  $\sum\sigma_p$  ( $E_{1/2} = 1.812 \sum\sigma_p + 0.045$ ,  $R^2 = 0.9784$ , plot ESI5†).

### Solid-state structures of *S,S'*-di-*tert*-butylferrocene-1,1'-disulfoxide derivatives

While Zhang and coll. already prepared *S,S'*-di-*tert*-butylferrocene-1,1'-disulfoxide and a few derivatives, their solid-state structures remained elusive up to now. In the frame of this study, we were able to grow crystals suitable for X-ray diffraction analysis for some compounds of interest. Compound **1** was found in a staggered conformation at the solid state, with the two *tert*-butyl moieties perpendicular to each Cp ring (Fig. 6). As a result of the *R* configuration of both sulfinyl

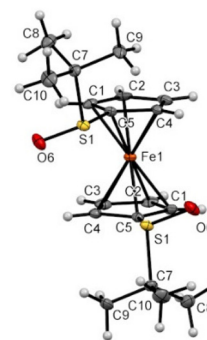


Fig. 6 Molecular structure of the compound **1** (thermal ellipsoids shown at the 30% probability level). Selected lengths [Å] and angles (°): C5–S1 1.758(4), C5–Cg1...Cg1–C5 –37.64(0.35) (Cg1 being the centroid of the C1–C2–C3–C4–C5 ring), C1–C5–S1–O6 18.5(4), C1–C5–S1–C7 –92.1(4), O6–S1...S1–O6 175.75(0.28).

groups, the two S=O bonds are pointing in opposite directions and both are slightly bent towards the iron atom.

The introduction of fluorine atoms next to each sulfoxide was almost without impact on the solid-state structure. Indeed, the compound **2d** also adopted a staggered conformation, with the two S=O bonds bent towards the iron and opposite to each other (Fig. 7). However, replacing the small fluorine atom by a bulkier trimethylsilyl group induced more changes. Indeed, the two S=O bonds in compound **2f** were still observed pointing in opposite directions, but with one close to coplanarity with the Cp ring (Fig. 8). Furthermore, probably due to the bulkiness of the silyl group, the *tert*-butyl moieties were found more bent than in compound **1** (−98.5° and −105.9° torsion angles compared to −92.1°). The ferrocene core further adopts an eclipsed conformation with the two silyl groups pointing in opposite directions. In addition to the  $pK_a$  calculation already discussed, the solid-state structure of ferrocene **2f** also helps to rationalize the regioselectivity observed during deprotonation experiments. Indeed, the positions adjacent to the trimethylsilyl groups are protected by these bulky substituents. However, the sulfinyl oxygen is well

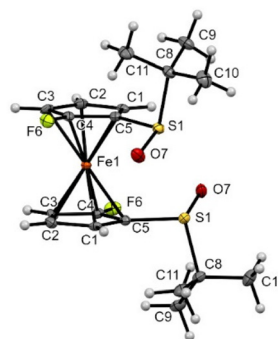
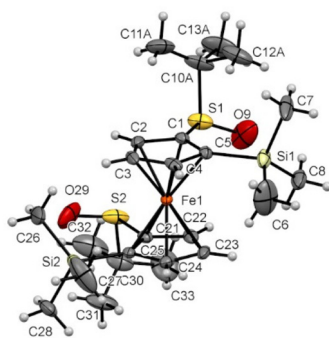


Fig. 7 Molecular structure of the compound **2d** (thermal ellipsoids shown at the 30% probability level). Selected lengths [Å] and angles (°): C5–S1 1.776(4), C4–F6 1.342(3), C5–Cg1...Cg1–C5 –43.56(0.33) (Cg1 being the centroid of the C1–C2–C3–C4–C5 ring), C4–C5–S1–C8 –89.6(4), O7–S1...S1–O7 175.6(2), F6–C4...C4–F6 168.3(3).







**Fig. 8** Molecular structure of the compound **2f** (thermal ellipsoids shown at the 30% probability level). Selected lengths [Å] and angles (°): C1–S1 1.770(3), C5–Si1 1.883(3), C21–S2 1.7770(3), C25–Si2 1.883(3), C1–Cg1...Cg2–C21 12.91(0.23) (Cg1 being the centroid of the C1–C2–C3–C4–C5 ring, Cg2 being the centroid of the C21–C22–C23–C24–C25 ring), C25–C21–S2–O29 5.7(4), C5–C1–S1–O9 15.2(4), C5–C1–S1–C10A –98.5(4), C25–C21–S2–C30 –105.9(3), O9–S1...S2–O29 161.51(0.28), Si1–C5...C25–Si2 132.73(0.18).

positioned to stabilize a lithiated intermediate at the 4 or 5 position of the opposite Cp ring until subsequent electrophilic trapping.

Although not as bulky as the trimethylsilyl group, the hydroxymethyl moiety induced more changes at the solid state (compound **3**, Fig. 9). Indeed, the presence of the two primary alcohols leads to the establishment of two intramolecular hydrogen bonds between a hydroxyl and the oxygen of a remote sulfinyl group acting as an acceptor. The hydrogen bond lengths and angles are within the expected range.<sup>126</sup> As a result, an eclipsed conformation was observed, with both S=O now pointing in the same direction, to lead to an O–S...S–O torsion angle of 35.26°. However, these bonds are also bent towards the iron atom with a torsion angle value of 19.6° while the *tert*-butyl groups are still perpendicular to their respective Cp rings. For comparison, the solid-state structure of the alcohol **R<sub>P</sub>-2c** has also been investigated and an intramolecular hydrogen bond has been similarly identified (see ESI†).

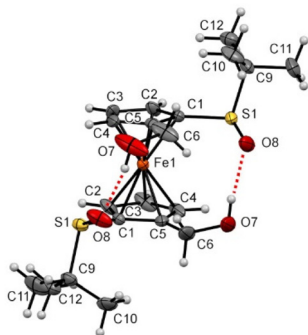


**Fig. 9** Molecular structure of the compound **3** (thermal ellipsoids shown at the 30% probability level). Selected lengths [Å] and angles (°): C1–S1 1.759(3), C5–C6 1.500(6), C5–Cg1...Cg2–C5 –14.33(0.33) (Cg1 being the centroid of the C1–C2–C3–C4–C5 ring, Cg2 being the centroid of the C21–C22–C23–C24–C25 ring), C1–C5–S1–C7 –92.1(4), O8–S1...S1–O8 35.26(0.28), H7...O8 1.98(0.07), O7–H7...O8 171.93(7.27), H7...O8–S1 121.67(2.12).

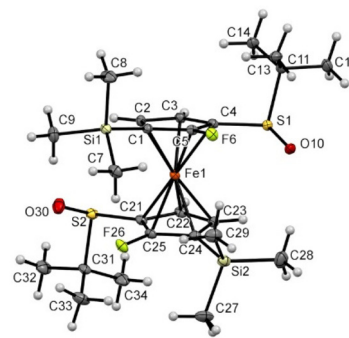


**Fig. 10** Molecular structure of the compound **8a** (thermal ellipsoids shown at the 30% probability level). Selected lengths [Å] and angles (°): C4–S1 1.772(3), C5–F6 1.346(3), C1–Si1 1.871(3), C21–S2 1.774(3), C25–F26 1.342(3), C24–Si2 1.874(3), C5–Cg1...Cg2–C24 –0.59(0.18) (Cg1 being the centroid of the C1–C2–C3–C4–C5 ring, Cg2 being the centroid of the C21–C22–C23–C24–C25 ring), mean plane C1–C2–C3–C4–C5...mean plane C21–C22–C23–C24–C25 9.31, mean plane C1–C2–C3–C4–C5...mean plane C4–S1C11 89.9, mean plane C21–C22–C23–C24–C25...mean plane C21–S2–C31 86.0, C5–C4–S1–O10 18.7(3), C25–C21–S2–O30 26.2(3), C5–C4–S1–C11 –92.6(3), C25–C21–S2–C31 –85.1(3); O10–S1...S2–O30 76.15(0.15), Si1–C1...C24–Si2 –62.33(0.18).

The hexasubstituted ferrocene **8a** was also found in an almost perfectly eclipsed conformation, probably to reduce the steric hindrance between the two trimethylsilyl substituents at the 3 and 3' positions (Fig. 10). However, the proximity of these bulky groups also induced the tilting of the Cp rings, with the C5–F6 bond inclined upwards. The two S=O bonds are observed pointing in the same direction, both bent towards the iron atom, with *tert*-butyl groups almost perpendicular to their respective Cp rings.

From the ferrocene **2f**, the introduction of an iodine atom at the 4 position (compound **6h**) induced minor changes on the solid-state structure (Fig. 11). Indeed, the ferrocene core

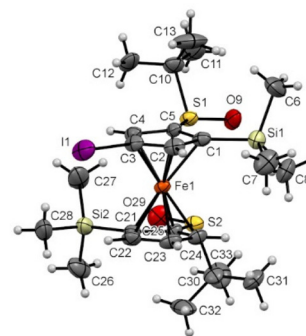


**Fig. 11** Molecular structure of the compound **6h** (thermal ellipsoids shown at the 30% probability level). Selected lengths [Å] and angles (°): C5–S1 1.776(6), C1–Si1 1.853(7), C3–I1 2.070(7), C25–S2 1.778(6), C21–Si2 1.895(7), C5–Cg1...Cg2–C25 4.82(0.43) (Cg1 being the centroid of the C1–C2–C3–C4–C5 ring, Cg2 being the centroid of the C21–C22–C23–C24–C25 ring), C1–C5–S1–O9 –2.0(6), C21–C25–C2–O29 3.2(6), C1–C5–S1–C10 –113.1(6), C21–C25–S2–C30 –108.9(6), O9–S1...S2–O29 –142.82(0.34), Si1–C1...C21–Si2 –147.09(0.39).



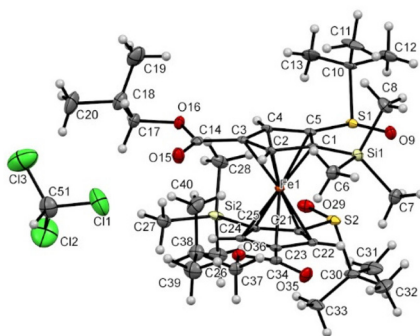


**Fig. 12** Molecular structure of the compound **6c** (thermal ellipsoids shown at the 30% probability level). Selected lengths [Å] and angles ( $^{\circ}$ ): C5–S1 1.780(4), C1–Si1 1.884(6), C3–C14 1.469(8), C21–S2 1.771 (5), C25–Si2 1.887 (6), C23–C34 1.477(8), C5–Cg1...Cg2–C21 –13.40(0.45) (Cg1 being the centroid of the C1–C2–C3–C4–C5 ring, Cg2 being the centroid of the C21–C22–C23–C24–C25 ring), C1–C5–S1–O9 –1.7(6), C25–C21–S2–O29 3.0(6), C1–C5–S1–C10 –112.9(6), C25–C21–S2–C30 –108.5(6), O9–S1...S2–O29 –160.34(0.27), Si1–C1...C25–Si2 –169.18(0.35), Cl1...O15 3.078(0.005), C51–Cl1...O15 138.34(0.38), Cl1...O15–C14 145.71(0.45).

was also found in an eclipsed conformation with the two S=O bonds pointing in opposite directions. However, both of them were almost coplanar with the Cp ring they are attached to ( $-2.0^{\circ}$  and  $3.2^{\circ}$  torsion angle) and the *tert*-butyl groups were also more bent away from the silyl groups.

A similar solid-state structure was finally determined for the compound **6c** having one isopropyl ester at the 4 position of each Cp ring (Fig. 12). It features an eclipsed conformation for the ferrocene, two S=O bonds pointing in opposite directions, the silyl groups almost opposite (Si1–C1... C25–Si2 torsion angle of  $-169.18(0.35)^{\circ}$ ) and two slightly bent downwards. A molecule of chloroform co-crystallized with our compound and a weak interaction between a chlorine atom and one of the esters was also observed.

## Conclusions

Although many ferrocenesulfoxide derivatives have been prepared over the last decades, the behaviour of (*R,R*)-*S,S'*-di-*tert*-butylferrocene-1,1'-disulfoxide and its derivatives in deprotonation have never been studied in details. Here, we found that the trends of regioselectivity observed with the 1,2- and 1,1'-disubstituted ferrocenes do not consistently apply to the functionalization of more hindered substrates such as 1,1',2,2'-tetrasubstituted derivatives. Thus, while a 2,2'-difluorinated derivative could be 3,3'-difunctionalized, the corresponding 2,2'-di(phenylthio) and 2,2'-bis(trimethylsilyl) substrates were instead 4,4'-difunctionalized.

While structural data were informative in explaining these results, additional  $pK_a$  calculations helped us gain a more detailed understanding of reactivity trends. Further functionalization by deprotonation-electrophilic trapping sequences was also possible, affording the first enantiopure

1,1',2,2',4,4'-hexa, 1,1',2,2',3,3'-hexa, 1,1',2,2',3,3',4,4'-octa, nona and even decasubstituted ferrocenes. The understanding of the key parameters allowing the synthesis and the control of the properties of these original compounds is fundamental for the development of molecules tailored for applications. Therefore, we hope that this first general study will be valuable in achieving this goal.

## Author contributions

Investigation, M. W., W. E., J.-P. H., M. B., T. R., Y. S. H. and V. E. M.; funding acquisition, project administration and supervision, W. E.; writing – original draft preparation, W. E., F. M., M. W., J.-P. H. and Y. S. H.; writing – review and editing, W. E., F. M., M. W., J.-P. H., Y. S. H., T. R., V. E. M. and O. A. I.

## Conflicts of interest

There are no conflicts to declare.

## Acknowledgements

This work was funded, in part, by the Agence Nationale de la Recherche (Ferrodance project). A CC-BY public copyright licence has been applied by the authors to present document and will be applied to all subsequent versions up to the Authors Accepted Manuscript arising from this submission, in accordance with the grant's open access conditions. This work was also supported by the Université de Rennes 1 and CNRS. We gratefully acknowledge the Fonds Européen de Développement Régional (FEDER; D8 VENTURE Bruker AXS diffractometer) and Thermofisher (generous gift of 2,2,6,6-tetramethylpiperidine).

## References

- 1 T. J. Kealy and P. L. Pauson, *Nature*, 1951, **168**, 1039.
- 2 S. A. Miller, J. A. Tebboth and J. F. Tremaine, *J. Chem. Soc.*, 1952, 632.
- 3 D. Astruc, *Eur. J. Inorg. Chem.*, 2017, 6.
- 4 A. Togni and T. Hayashi, *Ferrocenes: Homogeneous Catalysis, Organic Synthesis, Materials Science*, Wiley-VCH, Weinheim, Germany, 1995.
- 5 T. J. Colacot, *Chem. Rev.*, 2003, **103**, 3101.
- 6 R. Gómez-Arrayás, J. Adrio and J. C. Carretero, *Angew. Chem., Int. Ed.*, 2006, **45**, 7674.
- 7 N. A. Butt, D. Liu and W. Zhang, *Synlett*, 2014, 615.
- 8 M. Patra and G. Gasser, *Nat. Rev. Chem.*, 2017, **1**, 0066.
- 9 G. Jaouen, A. Vessières and S. Top, *Chem. Soc. Rev.*, 2015, **44**, 8802.
- 10 Y. C. Ong, S. Roy, P. C. Andrews and G. Gasser, *Chem. Rev.*, 2019, **119**, 730.



- 11 Y. Lin, H. Betts, S. Keller, K. Cariou and G. Gasser, *Chem. Soc. Rev.*, 2021, **50**, 10346.
- 12 B. Sharma and V. Kumar, *J. Med. Chem.*, 2021, **64**, 16865.
- 13 B. Zhou, L. Liu, P. Cai, G. Zeng, X. Li, Z. Wen and L. Chen, *J. Mater. Chem. A*, 2017, **5**, 22163.
- 14 M.-L. Hu, M. Abbasi-Azad, B. Habibi, F. Rouhani, H. Moghanni-Bavil-Olyaei, K.-G. Liu and A. Morsali, *ChemPlusChem*, 2020, **85**, 2397.
- 15 Z. Wei, D. Wang, Y. Liu, X. Guo, Y. Zhu, Z. Meng, Z.-Q. Yu and W.-Y. Wong, *J. Mater. Chem. C*, 2020, **8**, 10774.
- 16 L. Li, J. Zhang, C. Yang, L. Huang, J. Zhang, J. Bai, C. Redshaw, X. Feng, C. Cao, N. Huo, J. Li and B. Z. Tang, *Small*, 2021, **17**, 2103125.
- 17 G. G. A. Balavoine, J. C. Daran, G. Iftime, E. Manoury and C. Moreau-Bossuet, *J. Organomet. Chem.*, 1998, **567**, 191.
- 18 R. C. J. Atkinson, V. C. Gibson and N. J. Long, *Chem. Soc. Rev.*, 2004, **33**, 313.
- 19 I. R. Butler, *Eur. J. Inorg. Chem.*, 2012, 4387.
- 20 D. Schaarschmidt and H. Lang, *Organometallics*, 2013, **32**, 5668.
- 21 H. Butenschön, *Synthesis*, 2018, 3787.
- 22 M. Korb and H. Lang, *Eur. J. Inorg. Chem.*, 2022, e202100946.
- 23 W. Erb and F. Mongin, *Synthesis*, 2019, 146.
- 24 E. Lerayer, L. Radal, T. A. Nguyen, N. Dwadnia, H. Cattey, R. Amardeil, N. Pirio, J. Roger and J.-C. Hierso, *Eur. J. Inorg. Chem.*, 2020, 419.
- 25 G. Werner and H. Butenschön, *Organometallics*, 2013, **32**, 5798.
- 26 E. E. Bunel, L. Valle and J. M. Manriquez, *Organometallics*, 1985, **4**, 1680.
- 27 M. Malischewski, K. Seppelt, J. Sutter, D. Munz and K. Meyer, *Angew. Chem., Int. Ed.*, 2018, **57**, 14597.
- 28 I. Emme, S. Redlich, T. Labahn, J. Magull and A. De Meijere, *Angew. Chem., Int. Ed.*, 2002, **41**, 786.
- 29 M. D. Rausch, W. M. Tsai, J. W. Chambers, R. D. Rogers and H. G. Alt, *Organometallics*, 1989, **8**, 816.
- 30 K. Sünkel and S. Bernhartzeder, *J. Organomet. Chem.*, 2011, **696**, 1536.
- 31 D. W. Slocum, S. Duraj, M. Matusz, J. L. Cmarik, K. M. Simpson and D. A. Owen, *Met.-Containing Polym. Syst.*, 1985, 59.
- 32 P. Jutzi, C. Batz, B. Neumann and H.-G. Stammer, *Angew. Chem., Int. Ed. Engl.*, 1996, **35**, 2118.
- 33 K. Sünkel, S. Weigand, A. Hoffmann, S. Blomeyer, C. G. Reuter, Y. V. Vishnevskiy and N. W. Mitzel, *J. Am. Chem. Soc.*, 2015, **137**, 126.
- 34 W. Erb, N. Richy, J.-P. Hurvois, P. J. Low and F. Mongin, *Dalton Trans.*, 2021, **50**, 16933.
- 35 S. Bernhartzeder and K. Sünkel, *J. Organomet. Chem.*, 2012, **716**, 146.
- 36 F. L. Hedberg and H. Rosenberg, *J. Am. Chem. Soc.*, 1973, **95**, 870.
- 37 V. I. Boev and A. V. Dombrovskii, *Zh. Obshch. Khim.*, 1977, **47**, 727.
- 38 Y.-H. Han, M. J. Heeg and C. H. Winter, *Organometallics*, 1994, **13**, 3009.
- 39 I. R. Butler, *Inorg. Chem. Commun.*, 2008, **11**, 484.
- 40 S. M. Rumpf, I. S. Dimitrova, G. Schroeder and M. Malischewski, *Organometallics*, 2022, **41**, 1261.
- 41 T. Blockhaus, C. Klein-Heßling, P. M. Zehetmaier, F. L. Zott, H. Jangra, K. Karaghiosoff and K. Sünkel, *Chem. – Eur. J.*, 2019, **25**, 12684.
- 42 R. Broussier, S. Ninoreille, C. Bourdon, O. Blacque, C. Ninoreille, M. M. Kubicki and B. Gautheron, *J. Organomet. Chem.*, 1998, **561**, 85.
- 43 G. Trouve, R. Broussier, B. Gautheron and M. M. Kubicki, *Acta Crystallogr., Sect. C: Cryst. Struct. Commun.*, 1991, **47**, 1966.
- 44 M. Roemer, B. W. Skelton, M. J. Piggott and G. A. Koutsantonis, *Dalton Trans.*, 2016, **45**, 18817.
- 45 K. H. Taylor, S. E. Kalman, T. B. Gunnoe and M. Sabat, *Organometallics*, 2016, **35**, 1978.
- 46 S. Zürcher, V. Gramlich, D. von Arx and A. Togni, *Inorg. Chem.*, 1998, **37**, 4015.
- 47 T. Blockhaus, S. Bernhartzeder, W. Kempinger, C. Klein-Hessling, S. Weigand and K. Sünkel, *Eur. J. Org. Chem.*, 2020, 6576.
- 48 T. Hatanaka, Y. Ohki and K. Tatsumi, *Angew. Chem., Int. Ed.*, 2014, **53**, 2727.
- 49 H. Bauer, J. Weismann, D. Saurenz, C. Färber, M. Schär, W. Gidt, I. Schädlich, G. Wolmershäuser, Y. Sun, S. Harder and H. Sitzmann, *J. Organomet. Chem.*, 2016, **809**, 63.
- 50 C. J. Miller and D. O'Hare, *J. Mater. Chem.*, 2005, **15**, 5070.
- 51 D. A. Khobragade, S. G. Mahamulkar, L. Pospíšil, I. Císařová, L. Rulišek and U. Jahn, *Chem. – Eur. J.*, 2012, **18**, 12267.
- 52 S. Toma and R. Šebesta, *Synthesis*, 2015, 1683.
- 53 S. D. Waniek, J. Klett, C. Förster and K. Heinze, *Beilstein J. Org. Chem.*, 2018, **14**, 1004.
- 54 F. O. Arp and G. C. Fu, *J. Am. Chem. Soc.*, 2006, **128**, 14264.
- 55 X. Wang, R. Fröhlich, C. G. Daniliuc, B. Rieger, A. Jonovic, G. Kehr and G. Erker, *Organometallics*, 2012, **31**, 6741.
- 56 C. J. Richards and A. J. Locke, *Tetrahedron: Asymmetry*, 1998, **9**, 2377.
- 57 W.-P. Deng, V. Snieckus and C. Metallinos, in *Chiral Ferrocenes in Asymmetric Catalysis: Synthesis and Applications*, ed. L.-X. Dai and X.-L. Hou, Wiley-VCH, Weinheim, 2010, ch. 2, pp. 15–53.
- 58 B. F. Bonini, M. Fochi and A. Ricci, *Synlett*, 2007, 360.
- 59 T. Hayashi, T. Mise, M. Fukushima, M. Kagotani, N. Nagashima, Y. Hamada, A. Matsumoto, S. Kawakami, M. Konishi, K. Yamamoto and M. Kumada, *Bull. Chem. Soc. Jpn.*, 1980, **53**, 1138.
- 60 B. Pugin and X. Feng, WO2006-EP61861,2006114438, 2006.
- 61 M. Steurer, Y. Wang, K. Mereiter and W. Weissensteiner, *Organometallics*, 2007, **26**, 3850.
- 62 C. Ganter and T. Wagner, *Chem. Ber.*, 1995, **128**, 1157.



- 63 C. J. Richards and A. W. Mulvaney, *Tetrahedron: Asymmetry*, 1996, **7**, 1419.
- 64 K. H. Ahn, C.-W. Cho, H.-H. Baek, J. Park and S. Lee, *J. Org. Chem.*, 1996, **61**, 4937.
- 65 O. Riant, O. Samuel and H. B. Kagan, *J. Am. Chem. Soc.*, 1993, **115**, 5835.
- 66 H. Plenio, J. Hermann and A. Sehring, *Chem. – Eur. J.*, 2000, **6**, 1820.
- 67 J. Chiffre, Y. Coppel, G. G. A. Balavoine, J.-C. Daran and E. Manoury, *Organometallics*, 2002, **21**, 4552.
- 68 J. Niemeyer, G. Kehr, R. Fröhlich and G. Erker, *Dalton Trans.*, 2009, **38**, 3716.
- 69 B. Ferber, S. Top, R. Welter and G. Jaouen, *Chem. – Eur. J.*, 2006, **12**, 2081.
- 70 M. Steurer, K. Tiedl, Y. Wang and W. Weissensteiner, *Chem. Commun.*, 2005, **41**, 4929.
- 71 X. Feng, B. Pugin, B. Gschwend, F. Spindler, M. Paas and H.-U. Blaser, *ChemCatChem*, 2009, **1**, 85.
- 72 N. D'Antona, D. Lambusta, R. Morrone, G. Nicolosi and F. Secundo, *Tetrahedron: Asymmetry*, 2004, **15**, 3835.
- 73 D. Marquarding, H. Klusacek, G. Gokel, P. Hoffmann and I. Ugi, *J. Am. Chem. Soc.*, 1970, **92**, 5389.
- 74 W. Erb and F. Mongin, *Tetrahedron*, 2016, **72**, 4973.
- 75 W. Erb and T. Roisnel, *Chem. Commun.*, 2019, **55**, 9132.
- 76 F. Rebière, O. Riant, L. Ricard and H. B. Kagan, *Angew. Chem., Int. Ed. Engl.*, 1993, **32**, 568.
- 77 B. Ferber and H. B. Kagan, *Adv. Synth. Catal.*, 2007, **349**, 493.
- 78 D. H. Hua, N. M. Lagneau, Y. Chen, P. M. Robben, G. Clapham and P. D. Robinson, *J. Org. Chem.*, 1996, **61**, 4508.
- 79 O. Riant, G. Argouarch, D. Guillaneux, O. Samuel and H. B. Kagan, *J. Org. Chem.*, 1998, **63**, 3511.
- 80 J. Priego, O. García Mancheño, S. Cabrera, R. Gómez Arrayás, T. Llamas and J. C. Carretero, *Chem. Commun.*, 2002, **38**, 2512.
- 81 T. Sasamori, M. Sakagami, M. Niwa, H. Sakai, Y. Furukawa and N. Tokitoh, *Chem. Commun.*, 2012, **48**, 8562.
- 82 U. Caniparoli, I. Escofet and A. M. Echavarren, *ACS Catal.*, 2022, **12**, 3317.
- 83 N. M. Lagneau, Y. Chen, P. M. Robben, H.-S. Sin, K. Takasu, J.-S. Chen, P. D. Robinson and D. H. Hua, *Tetrahedron*, 1998, **54**, 7301.
- 84 M. Wen, W. Erb, F. Mongin, M. Blot and T. Roisnel, *Chem. Commun.*, 2022, **58**, 2002.
- 85 M. Wen, W. Erb, F. Mongin, Y. S. Halauko, O. A. Ivashkevich, V. E. Matulis and T. Roisnel, *Molecules*, 2022, **27**, 1798.
- 86 M. Raghunath, W. Gao and X. Zhang, *Tetrahedron: Asymmetry*, 2005, **16**, 3676.
- 87 M. D. Rausch and D. Ciappenelli, *J. Organomet. Chem.*, 1967, **10**, 127.
- 88 D. J. Weix and J. A. Ellman, *Org. Lett.*, 2003, **5**, 1317.
- 89 A. B. Fischer, J. B. Kinney, R. H. Staley and M. S. Wrighton, *J. Am. Chem. Soc.*, 1979, **101**, 6501.
- 90 N. Oguni and T. Omi, *Tetrahedron Lett.*, 1984, **25**, 2823.
- 91 M. Watanabe, N. Hashimoto, S. Araki and Y. Butsugan, *J. Org. Chem.*, 1992, **57**, 742.
- 92 H. Wally, M. Widhalm, W. Weissensteiner and K. Schlögl, *Tetrahedron: Asymmetry*, 1993, **4**, 285.
- 93 C. Bolm, N. Hermanns, J. P. Hildebrand and K. Muniz, *Angew. Chem., Int. Ed.*, 2000, **39**, 3465.
- 94 T. Ahern, H. Müller-Bunz and P. J. Guiry, *J. Org. Chem.*, 2006, **71**, 7596.
- 95 W. Zhang, H. Yoshinaga, Y. Imai, T. Kida, Y. Nakatsujii and I. Ikeda, *Synlett*, 2000, 1512.
- 96 A. Voituriez, A. Panossian, N. Fleury-Brégeot, P. Retailleau and A. Marinetti, *J. Am. Chem. Soc.*, 2008, **130**, 14030.
- 97 A. Voituriez, A. Panossian, N. Fleury-Brégeot, P. Retailleau and A. Marinetti, *Adv. Synth. Catal.*, 2009, **351**, 1968.
- 98 M. Neel, A. Panossian, A. Voituriez and A. Marinetti, *J. Organomet. Chem.*, 2012, **716**, 187.
- 99 B. A. Surgenor, L. J. Taylor, A. Nordheider, A. M. Z. Slawin, K. S. Athukorala Arachchige, J. D. Woollins and P. Kilian, *RSC Adv.*, 2016, **6**, 5973.
- 100 F. Horký, I. Císařová and P. Štěpnička, *Chem. – Eur. J.*, 2021, **27**, 1282.
- 101 W. Chen, W. Mbafor, S. M. Roberts and J. Whittall, *J. Am. Chem. Soc.*, 2006, **128**, 3922.
- 102 W. Erb, V. Carré and T. Roisnel, *Eur. J. Org. Chem.*, 2021, 5702.
- 103 F. Allouch, N. Dwadnia, N. V. Vologdin, Y. V. Svyaschenko, H. Cattley, M.-J. Penouilh, J. Roger, D. Naoufal, R. Ben Salem, N. Pirio and J.-C. Hierso, *Organometallics*, 2015, **34**, 5015.
- 104 S. Lee, J. H. Koh and J. Park, *J. Organomet. Chem.*, 2001, **637–639**, 99.
- 105 C. Pichon, B. Odell and J. M. Brown, *Chem. Commun.*, 2004, **40**, 598.
- 106 B. Marsh, C. Frost and D. Pearce, *WO Pat.*, WO2013190328, 2013.
- 107 M. Tazi, W. Erb, Y. S. Halauko, O. A. Ivashkevich, V. E. Matulis, T. Roisnel, V. Dorcet and F. Mongin, *Organometallics*, 2017, **36**, 4770.
- 108 M. Tazi, M. Hedidi, W. Erb, Y. S. Halauko, O. A. Ivashkevich, V. E. Matulis, T. Roisnel, V. Dorcet, G. Bentabed-Ababsa and F. Mongin, *Organometallics*, 2018, **37**, 2207.
- 109 W. Erb, M. Wen, J.-P. Hurvois, F. Mongin, Y. S. Halauko, O. A. Ivashkevich, V. E. Matulis and T. Roisnel, *Eur. J. Inorg. Chem.*, 2021, 3165.
- 110 M. Wen, W. Erb, F. Mongin, Y. S. Halauko, O. A. Ivashkevich, V. E. Matulis, T. Roisnel and V. Dorcet, *Organometallics*, 2021, **40**, 1129.
- 111 A. Škvorcová and R. Šebesta, *Org. Biomol. Chem.*, 2014, **12**, 132.
- 112 N. Mohammadi, A. Ganesan, C. T. Chantler and F. Wang, *J. Organomet. Chem.*, 2012, **713**, 51.
- 113 R. A. Brown, A. Houlton, R. M. G. Roberts, J. Silver and C. S. Frampton, *Polyhedron*, 1992, **11**, 2611.
- 114 T. J. Peckham, D. A. Foucher, A. J. Lough and I. Manners, *Can. J. Chem.*, 1995, **73**, 2069.



- 115 R. S. Laufer, U. Veith, N. J. Taylor and V. Snieckus, *Org. Lett.*, 2000, **2**, 629.
- 116 B. M. Trost and D. J. Murphy, *Organometallics*, 1985, **4**, 1143.
- 117 I. R. Butler, *Organometallics*, 2021, **40**, 3240.
- 118 M. Tazi, W. Erb, T. Roisnel, V. Dorcet, F. Mongin and P. J. Low, *Org. Biomol. Chem.*, 2019, **17**, 9352.
- 119 F. Mongin, E. Marzi and M. Schlosser, *Eur. J. Org. Chem.*, 2001, 2771.
- 120 A. Gref, P. Diter, D. Guillaneux and H. B. Kagan, *New J. Chem.*, 1997, **21**, 1353.
- 121 W. F. Little, C. N. Reilley, J. D. Johnson and A. P. Sanders, *J. Am. Chem. Soc.*, 1964, **86**, 1382.
- 122 X. You, C. Li, J. Chen, Q. Chao, X. Pen and A. Dai, *Kexue Tongbao*, 1987, **32**, 1410.
- 123 A. Hildebrandt, K. Al Khalyfeh, D. Schaarschmidt and M. Korb, *J. Organomet. Chem.*, 2016, **804**, 87.
- 124 M. S. Inkpen, S. Du, M. Hildebrand, A. J. P. White, N. M. Harrison, T. Albrecht and N. J. Long, *Organometallics*, 2015, **34**, 5461.
- 125 D. M. Evans, D. D. Hughes, P. J. Murphy, P. N. Horton, S. J. Coles, F. F. de Biani, M. Corsini and I. R. Butler, *Organometallics*, 2021, **40**, 2496.
- 126 D. Herschlag and M. M. Pinney, *Biochemistry*, 2018, **57**, 3338.

